

Testing theories of the glass transition with the same liquid, but many kinetic rules

Cristina Gavazzoni* and Carolina Brito†

*Instituto de Física, Universidade Federal do Rio Grande do Sul,
Caixa Postal 15051, CEP 91501-970, Porto Alegre, Rio Grande do Sul, Brazil*

Matthieu Wyart‡

Institute of Physics, Ecole Polytechnique Federale de Lausanne, 729 BSP UNIL, 1015, Lausanne, Switzerland

(Dated: February 28, 2024)

We study the glass transition by exploring a broad class of kinetic rules that can significantly modify the normal dynamics of super-cooled liquids, while maintaining thermal equilibrium. Beyond the usual dynamics of liquids, this class includes dynamics in which a fraction $(1 - f_R)$ of the particles can perform pairwise exchange or ‘swap moves’, while a fraction f_P of the particles can only move along restricted directions. We find that (i) the location of the glass transition varies greatly but smoothly as f_P and f_R change and (ii) it is governed by a linear combination of f_P and f_R . (iii) Dynamical heterogeneities (DH) are not governed by the static structure of the material, their magnitude correlates instead with the relaxation time. (iv) We show that a recent theory for temporal growth of DH based on thermal avalanches holds quantitatively throughout the (f_R, f_P) diagram. These observations are negative items for some existing theories of the glass transition, particularly those reliant on growing thermodynamic order or locally favored structure, and open new avenues to test other approaches, as we illustrate.

Understanding why liquids glass formers cease to flow near their glass transition T_g remains a challenge. At that point, the relaxation time τ_α beyond which stress relaxes is of order of minutes, which is fifteen decades larger than at high temperatures. From τ_α , the activation energy E_a can be defined as $\tau_\alpha = t_0 \exp(E_a/T)$, where t_0 is a microscopic time scale and T is the temperature (in the units of the Boltzmann constant). In liquids called fragile, E_a can increase five-fold or more under cooling [1–4]. As the dynamics slows down, it also becomes more and more heterogeneous, corresponding to a growing length scale ξ [5–8]. Contrasting theories seek to explain these two facts. In the first class of views, including Adam-Gibbs [9] and Random First Order Theory (RFOT) [10–12], the increase of activation energy stems from the emergence of some order on a growing length ξ , that must be destroyed by cooperative motion on that scale to relax the material. E_a can then be expressed in terms of purely thermodynamic quantities, independently of the kinetic rules governing the dynamics. Some real space approaches associate such a growing order to locally favored structures [13, 14]. A second viewpoint seeks to capture the mechanism of dynamical facilitation, whereby the relaxation of a given region speeds up the relaxation of regions nearby. Kinetically constrained models [15, 16], such as the East model, capture this effect and suggest a scenario [17–19] in which thermodynamics plays almost no role, but dynamics is heterogeneous and the growth of activation energy stems from non-local rearrangements taking place over ξ . At odds with these two views, a third approach that includes free volume [20] or elastic [21–24] models,

assumes that the activation energy is not controlled by a growing length scale. Instead, it is governed by the energy cost of elementary rearrangements of a few particles jumping over a barrier. The elastic coupling between rearrangements [25–33] leads to a correlated dynamics [34] that can be described in terms of avalanches of activated events [35].

Molecular dynamics simulations of models of super-cooled liquids have been extremely informative to characterize the glass transition [36], yet distinct views on this phenomenon have been hard to definitely contrast [12]. Our present goal is to show that for some popular models of liquids, a very broad class of kinetic rules can be considered, which can continuously (and very significantly) speed up or slow-down the normal dynamics, while preserving thermal equilibrium. Although these rules would be hard to implement in actual experiments, they are equivalent to dynamics with purely local rules, and as such theories of the glass transition should apply to them. This approach thus opens an avenue to test more stringently theories of glassy dynamics. Specifically, our work builds on ‘swap’ Monte Carlo algorithms. In these algorithms, pairs of particles can exchange positions, in addition to their usual translation moves [37–41]. For continuously polydisperse systems, these algorithms can speed up the dynamics by 15 orders of magnitude or more [41], and can change the glass transition temperature T_g by up to a factor of two. It allows one to explore glasses with a stability similar to that reached in experiments.

Our central result is to introduce a family of kinetic rules, where a fraction f_R of the particles cannot swap, and a fraction f_P of the particles can only move along randomly-chosen hyperplanes. We provide systematic measurements of the dynamics in the (f_R, f_P) diagram in two and three dimensions, that includes the normal

* crigava@gmail.com

† carolina.brito@ufrgs.br

‡ matthieu.wyart@epfl.ch

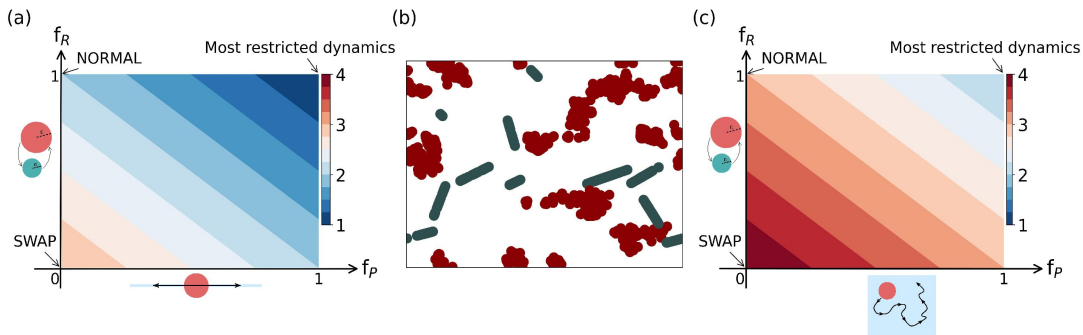


FIG. 1: Diagram indicating the number of degrees of freedom for spatial dimension $d = 2$ (a) and $d = 3$ (c) as a function of the fraction f_R of particles that cannot swap and the fraction f_P of particles whose translation motion is restricted. Panel (b) shows the particles positions at various time points within some time interval for $d = 2$. Particles that can move freely in all direction are shown in red, and particles that are restricted to linear motion appear in blue. For $d = 3$, this constraint is more gentle, as particles can still move on planes as sketched in (c).

dynamics $(1, 0)$ as well as swap $(0, 0)$. Overall, our observations are negative items for theories based on a growing thermodynamic order. We discuss how devoted studies could be used in these models to test alternative views of the glass transition.

Changing continuously the kinetic rules of liquids:

Swap moves lead to a considerable speed up of the dynamics [37, 40, 41]. Importantly, despite its apparent non-local character, swap dynamics can be conceived as a purely local dynamics. Following [37, 42, 43], swap is equivalent to considering identical particles endowed with an additional ‘breathing’ degree of freedom, allowing them to change their size according to some chemical potential $\mu(R)$. Indeed, letting pairs of particles exchange is equivalent, in the thermodynamic limit, to letting individual particles exchange with a bath of particles of all possible sizes R . $\mu(R)$ is then chosen to obtain the desired polydispersity, which is continuous for continuously poly-disperse particles [37, 42]. Adding such a degree of freedom per particle dramatically softens the energy landscape [42, 44–46] while preserving thermodynamic and structural properties. It also affects the dynamics: following the center of the particles, and considering that a swap move corresponds to a change of the size of two particles but not of their position, leads to the following observation. Dynamical correlations grow under cooling as for the normal dynamics, but the correlation length starts growing at a much smaller temperature [41]. To study more systematically such effects and their consequences, following [47] we vary the parameter $f_R \in [0, 1]$, characterizing the number of particles that cannot swap. Unlike [47], we do not consider that particles that swap positions perform a jump, as it leads to very different dynamics.

Following this logic, we propose to add even more kinetic constraints by restricting the motion of a fraction $f_P \in [0, 1]$ of the particles, as illustrated in Fig.1. Each such particle is forbidden to move along one random direction associated to it, and for an infinite system

they would be each confined along a random hyperplane. Overall, the number of degrees of freedom for a system of N particles is then $N(d - f_P + 1 - f_R)$. Note that for the periodic boundary condition we consider below, this dynamics is ergodic as such hyperplanes visit the neighborhood of any point with probability one, if their orientation is randomly chosen. For dynamics that satisfy detailed balance like ours, it ensures that thermal equilibrium will eventually be reached. Thus structural and thermodynamic properties are only governed by ϕ , independently of the choices of kinetic rules embodied in (f_R, f_P) . Note that other procedures were proposed to reduce the number of degrees of freedom, such as pinning particles starting from an equilibrated system as proposed e.g. in [48]. Yet in that case ergodicity is obviously broken once pinned particles are chosen, and the dynamical properties of the system are not translation-invariant anymore.

In the present work, we specifically perform Monte Carlo simulations of systems with N continuously poly-disperse hard spheres particles of packing fraction ϕ in a regular box of linear size L , with periodic boundary conditions. For hard particles, instead of temperature, ϕ is the good controlled parameter. The choice of polydispersity together with other numerical details are shown in the Appendix A. Figure 1-(a,c) shows a schematic diagram of the different dynamics we explore in $d = 2$ and $d = 3$ respectively, and indicate in color the associated number of degrees of freedom. Figure1-(b) illustrates an example of the particles trajectories at a short time for $d = 2$, revealing which particles are restricted to linear motion, and which ones are not.

Dependence of the glass transition packing fraction ϕ_G with kinetic rules: For $d = 3$, our choice of polydispersity and Monte-Carlo algorithm follows closely previous works [41, 49], where it was shown that swap can speed up the dynamics by 15 decades or more. Here we observe a giant speed up of swap in our $d = 2$ system as well, as documented in Appendix B. We consider the dynamics on

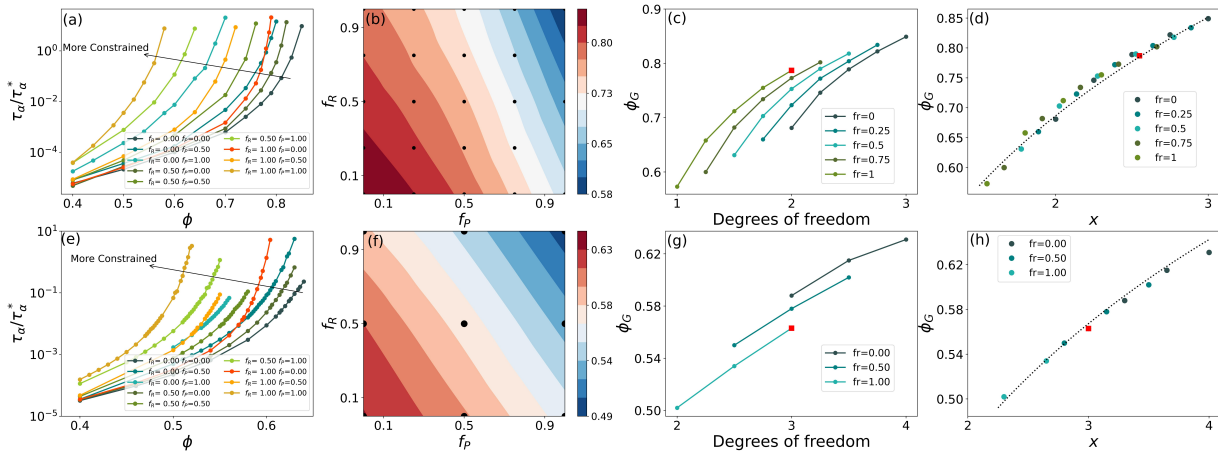


FIG. 2: $\tau_\alpha/\tau_\alpha^*$ as function of ϕ for different values of f_R and f_P for $d = 2$ (a) and $d = 3$ (e). From these curves, ϕ_G as a function of f_R and f_P is extracted, as indicated in color for $d = 2$ (b) and $d = 3$ (f). The discs mark the simulation data, from which extrapolations are made. (c,g) show ϕ_G as a function of the number of degrees of freedom per particle $d + 1 - f_R - f_P$ and (d,h) show that ϕ_G can be collapsed as a function of an effective number of constraints $x = f_P + C(d)f_R$, with $C(2) = 0.45$, and $C(3) = 0.70$. The normal dynamics is marked as a red square in these plots.

the full phase diagram (f_R, f_P) . Fig.2-(a,e) show τ_α vs ϕ for such dynamics as the parameters (f_R, f_P) are varied, both for $d = 2$ and $d = 3$. Fig.2-(b,f) represents the corresponding value of ϕ_G in color, as extrapolated from the different measurements made as indicated by circles. The most remarkable results are that (i) ϕ_G varies very significantly, and continuously throughout the phase diagram. In particular, there is no evidence for a region surrounding the normal dynamics where kinetic constraints would not matter and ϕ_G would plateau. The normal dynamics can be made continuously faster or slower. (ii) Observing these two diagrams, it is apparent that most of the variation of ϕ_G is captured by a linear combination of f_R and f_P . This hypothesis is tested in Fig.2-(d,h), where it is shown that $\phi_G(f_R, f_P) = \phi_G(x)$, where x can be thought of as an effective number of constraints $x = f_P + C(d)f_R$, where the coefficient $C(d) \leq 1$ characterizes the relative effect of breathing degrees of freedom *v.s.* translational ones. (iii) qualitative observations are independent of the spatial dimension d .

Dynamical heterogeneities are not governed by structural properties: Various theoretical approaches propose that dynamical heterogeneities are controlled by equilibrated structural properties, such as the extension of locally-favored structure [13, 14] or a point to set length [11, 12] entering RFOT (although additional effects such as facilitation can be added to this theory to increase further dynamical correlations, see e.g. [50] for a recent discussion). In our set-up, these properties depend only on ϕ , and not on the values of parameters f_R, f_P . Here instead we find that for the relaxation times we can probe and the system we consider, the dynamical susceptibility χ_4 characterizing the magnitude of dynamical heterogeneities are not governed by ϕ only, but instead depend strongly on f_R, f_P as illustrated in Fig.3(a). Much less

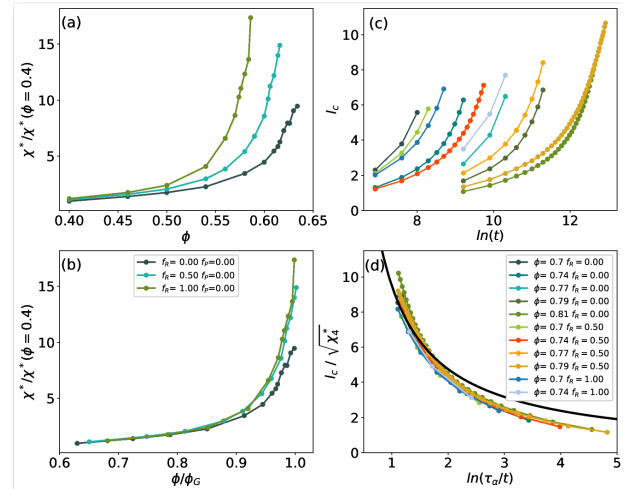


FIG. 3: (a) Maximum χ_4^* of the dynamic susceptibility $\chi_4(t)$ for $d = 3$ as a function of ϕ as f_R is varied indicated in legend, and $f_P = 0$. (b) $\chi_4^*/\chi_4^*(\phi = 0.4)$ as a function of ϕ/ϕ_G . Comparing (a) and (b) reveals that ϕ/ϕ_G is a much better predictor of DH than ϕ . (c) Coarsening length l_c for $d = 2$ *v.s.* $\ln(t)$ as ϕ is varied, for different values of f_R indicated in legend (d) for $f_P = 0$ and $t \leq \tau_\alpha/3$. (d) l_c collapses when axis are rescaled as predicted by Eq.1. The full black line is the theoretical prediction $l_c = a\sqrt{\chi_4^*}[\ln(\tau_\alpha/t)]^{-1}$ with $a = 9.5$.

variation in χ_4 is found when plotted as a function of ϕ/ϕ_G as shown in Fig.3(b).

These results indicate that heterogeneities are not controlled by a length scale that would directly appear in the structure. Indeed, dynamical correlations are small for the swap dynamics at significant packing fraction for

which the normal dynamics is already very correlated [41]. Thus, although locally favored structure may affect dynamical heterogeneities in specific systems (such as two-dimensional systems of discs that can display hexatic order [14]), it does not appear to be the case for continuously polydisperse particles, at least in the range of time scale that can be probed numerically.

The temporal evolution of DH follows that of thermal avalanches: Starting from a reference equilibrated configuration, coloring rearranging regions reveals a coarsening phenomenon [51, 52] and a growing length scale $l_c(t)$, as shown in Fig.3. Quantitatively we define $l_c(t) = \langle l^3 \rangle_t / \langle l^2 \rangle_t$ where the average $\langle \cdot \rangle_t$ is made on all clusters of connected relaxed particles at time t , and l is the square root of the number of particles involved in a cluster. In [35], a description of this coarsening based on facilitation via thermal avalanches of local activated rearrangements was proposed. It was refined and also argued to apply to creep flows in elastic manifolds in [53], and implies for $t \ll \tau_\alpha$ and l_c much smaller than the system size:

$$l_c \sim \xi [\ln(\tau_\alpha/t)]^{-1/(\tilde{\sigma}\tilde{d}_f)} \quad (1)$$

where ξ is the correlation length, $\tilde{\sigma}$ some exponent and \tilde{d}_f is the fractal dimension of the clusters. In this view, $\xi^{\tilde{d}_f} \sim \chi_4^*$ which characterizes the typical cluster volume. For $d = 2$, $\tilde{d}_f \approx 2$ and $\tilde{\sigma} \approx 1/2$ [35], leading to $l_c \sim \sqrt{\chi_4^*} [\ln(\tau_\alpha/t)]^{-1}$. As shown in Fig.3(d), this prediction works remarkably well, independently of f_R . It supports that thermal avalanches cause DH independently of the kinetic rules chosen.

Discussion: Swap Monte Carlo algorithms can be restricted to local moves with no significant effects on the dynamics [41]. More fundamentally, they are equivalent to a purely local kinetic rule where particles can adapt their radii [37, 42]. For theories based on a growing order on some length ξ_{coop} such as RFOT, or approaches based on locally favored structures, barriers are cooperative and can be expressed in terms of thermodynamic quantities alone. They should be present for any local kinetic rules [46], including those studied here. Thus in these approaches, the core mechanism slowing down the dynamics near the glass transition should not depend on the choice of (f_R, f_P) . Authors in [54] acknowledged that swap and normal dynamics should asymptotically relax at the same pace according to RFOT, but countered that pre-asymptotic corrections (not currently described within this theory) may cause the observed difference.

The main difficulty with this view is that the dynamics is very different as the parameters (f_R, f_P) change: as shown in Fig.5, these dynamics do not become equivalent even after a slowing down of 15 decades accessible experimentally. To have predictive power, RFOT or theories based on thermodynamic quantities should specify a value for the parameters (f_R, f_P) for which they apply. However, currently they don't. Our observation that ϕ_G continuously depends on (f_R, f_P) , and does not

plateau to some constant value around the normal dynamics $(1, 0)$, shows that the normal dynamics is just one among many other dynamics. This point underlines the lack of predictive power of RFOT or related theories - at least for the systems of continuously polydisperse particles studied here.

By contrast, for theories based on kinetic constraints or on local barriers (known to depend on kinetic rules [42]), the fact that ϕ_G should continuously vary with the amount of constraints is evident. The normal dynamics is slower simply because it is a kinetically constrained version of swap dynamics.

Conclusion: RFOT is a mean-field theory of the glass transition, which has shown undeniable successes. It is exact in infinite dimension [55, 56], correctly captures aspects of the thermodynamics of super-cooled liquids [57], and presents a dynamical transition [11, 58, 59] akin to mode coupling theory, that describes some aspects of liquid dynamics at intermediate temperatures [60]. Yet our results support that its description of activation near the glass transition does not apply for the continuously polydisperse systems studied here. Although our conclusions are restricted to these specific systems where swap is so performant, these models are known to capture the key facts associated with the glass transition [52].

The model we introduced, with its very large variation of dynamics with different kinetic rules, offers new opportunities to test different theories of the glass transition, extending previous observations that were only considered for a single kinetic rule. As an illustration, we showed that the time evolution of dynamical heterogeneities follow a description of facilitation based on thermal avalanches of local rearrangements [35] independently of the kinetic rules chosen, emphasizing the robustness of this theory. Other debated issues that this model would help resolve include what observable predicts best the regions which will flow first, the so-called dynamical propensity, for which many candidates were proposed [23, 61–63]. Likewise, numerical tests put forward to test theories of the slowing down of the dynamics (i.e. how the activation energy E_a depends on temperature or packing fraction) can now be made much more stringent. The list includes kinetically constrained or lattice gas models [64], that can be tested by analyzing irreversible events [65]. Furthermore, the notion that glassy dynamics correspond to local rearrangements was supported by the measurement of the density of state of local barriers [24]; and these barriers were argued to be governed alternatively by global [21] or local [22] elasticity, or by the amplitude of vibrational motion [66]. Varying (f_R, f_P) in these measurements will indicate which viewpoint is most likely correct. Overall, we have added an axis to the glass transition problem by varying continuously kinetic rules, affecting strongly observations and giving a new handle to decide which theory of the glass transition actually applies.

ACKNOWLEDGMENTS

We thank the Simons collaboration for discussions, in particular L. Berthier, G. Biroli, M. Ozawa and C. Scalliet. We thank J.P. Bouchaud, T. deGeus, W. Ji, M.

Muller, M. Pica Ciamarra, M. Popovic, A. Tahei and A. Rosso for discussions, and J. Kurchan for exchanges at the beginning of this project. MW acknowledges support from the Simons Foundation Grant (No. 454953 Matthieu Wyart) and from the SNSF under Grant No. 200021-165509. C.B. and C.G. thank the Brazilian agency CAPES and CNPq for the financial support..

-
- [1] D. Anderson, *Science* **267**, 1618 (1995).
- [2] M. D. Ediger, C. A. Angell, and S. R. Nagel, *The journal of physical chemistry* **100**, 13200 (1996).
- [3] P. Debenedetti and F. Stillinger, *Nature* **410**, 259 (2001).
- [4] L. Berthier and G. Biroli, *Reviews of modern physics* **83**, 587 (2011).
- [5] W. Kob, C. Donati, S. J. Plimpton, P. H. Poole, and S. C. Glotzer, *Physical review letters* **79**, 2827 (1997).
- [6] R. Yamamoto and A. Onuki, *Physical Review E* **58**, 3515 (1998).
- [7] C. Dalle-Ferrier, C. Thibierge, C. Alba-Simionesco, L. Berthier, G. Biroli, J.-P. Bouchaud, F. Ladieu, D. L'Hôte, and G. Tarjus, *Phys. Rev. E* **76**, 041510 (2007).
- [8] S. Karmakar, C. Dasgupta, and S. Sastry, *Annu. Rev. Condens. Matter Phys.* **5**, 255 (2014).
- [9] G. Adam and J. H. Gibbs, *The journal of chemical physics* **43**, 139 (1965).
- [10] T. R. Kirkpatrick, D. Thirumalai, and P. G. Wolynes, *Physical Review A* **40**, 1045 (1989).
- [11] V. Lubchenko and P. G. Wolynes, *Annu. Rev. Phys. Chem.* **58**, 235 (2007).
- [12] G. Biroli and J.-P. Bouchaud, *Structural Glasses and Supercooled Liquids: Theory, Experiment, and Applications*, 31 (2012).
- [13] C. Patrick Royall, S. R. Williams, T. Ohtsuka, and H. Tanaka, *Nature materials* **7**, 556 (2008).
- [14] T. Kawasaki, T. Araki, and H. Tanaka, *Physical review letters* **99**, 215701 (2007).
- [15] F. Ritort and P. Sollich, *Advances in physics* **52**, 219 (2003).
- [16] L. Berthier, G. Biroli, J.-P. Bouchaud, L. Cipelletti, and W. van Saarloos, *Dynamical heterogeneities in glasses, colloids, and granular media*, Vol. 150 (OUP Oxford, 2011).
- [17] J. P. Garrahan and D. Chandler, *Physical review letters* **89**, 035704 (2002).
- [18] J. P. Garrahan, R. L. Jack, V. Lecomte, E. Pitard, K. van Duijvendijk, and F. van Wijland, *Physical review letters* **98**, 195702 (2007).
- [19] L. Hedges, R. Jack, J. Garrahan, and D. Chandler, *Science* **323**, 1309 (2009).
- [20] D. Turnbull and M. H. Cohen, *The Journal of chemical physics* **34**, 120 (1961).
- [21] J. Dyre, *Rev. Mod. Phys.* **78**, 953 (2006).
- [22] G. Kapteijns, D. Richard, E. Bouchbinder, T. B. Schröder, J. C. Dyre, and E. Lerner, *The Journal of Chemical Physics* **155**, 74502 (2021).
- [23] M. Lerbinger, A. Barbot, D. Vandembroucq, and S. Patinet, *Physical Review Letters* **129**, 195501 (2022).
- [24] M. P. Ciamarra, W. Ji, and M. Wyart, "The energy cost of local rearrangements, not cooperative effects, makes glasses solid," (2023).
- [25] A. Lemaître, *Phys. Rev. Lett.* **113**, 245702 (2014).
- [26] S. Chowdhury, S. Abraham, T. Hudson, and P. Harrowell, *The Journal of chemical physics* **144**, 124508 (2016).
- [27] H. Tong, S. Sengupta, and H. Tanaka, *Nature communications* **11**, 1 (2020).
- [28] B. Wu, T. Iwashita, and T. Egami, *Physical Review E* **91**, 032301 (2015).
- [29] M. Maier, A. Zippelius, and M. Fuchs, *Physical review letters* **119**, 265701 (2017).
- [30] D. Steffen, L. Schneider, M. Müller, and J. Rottler, *The Journal of Chemical Physics* **157**, 064501 (2022).
- [31] E. Flenner and G. Szamel, *Physical Review Letters* **114**, 025501 (2015).
- [32] L. Klochko, J. Baschnagel, J. Wittmer, H. Meyer, O. Benzerara, and A. Semenov, *The Journal of Chemical Physics* **156**, 164505 (2022).
- [33] R. Chacko, F. Landes, G. Biroli, O. Dauchot, A. Liu, and D. Reichman, *arXiv preprint 2103.01852* (2021), 10.48550/arXiv.2103.01852.
- [34] M. Ozawa and G. Biroli, *Physical Review Letters* **130**, 138201 (2023).
- [35] A. Tahaei, G. Biroli, M. Ozawa, M. Popović, and M. Wyart, *arXiv preprint arXiv:2305.00219* (2023).
- [36] W. Kob, *Journal of Physics: Condensed Matter* **11**, R85 (1999).
- [37] J. Briano and E. Glandt, *J. Chem. Phys.* **80**, 3336 (1984).
- [38] T. Grigera and G. Parisi, *Phys. Rev. E* **63**, 045102 (2001).
- [39] L. Fernández, V. Martín-Mayor, and P. Verrocchio, *Physical review letters* **98**, 085702 (2007).
- [40] R. Gutiérrez, S. Karmakar, Y. Pollack, and I. Procaccia, *Europhys. Lett.* **111**, 56009 (2015).
- [41] A. Ninarello, L. Berthier, and D. Coslovich, *Phys. Rev. X* **7**, 021039 (2017).
- [42] C. Brito, E. Lerner, and M. Wyart, *Phys. Rev. X* **8**, 031050 (2018).
- [43] V. F. Hagh, S. R. Nagel, A. J. Liu, M. L. Manning, and E. I. Corwin, *Proceedings of the National Academy of Sciences* **119**, e2117622119 (2022).
- [44] G. Szamel, *Journal of Statistical Mechanics: Theory and Experiment* **2019**, 104016 (2019).
- [45] H. Ikeda, P. Urbani, and F. Zamponi, *Journal of Physics A: Mathematical and Theoretical* **52**, 344001 (2019).
- [46] M. Wyart and M. Cates, *Phys. Rev. Lett.* **119**, 195501 (2017).
- [47] G. Gopinath, C.-S. Lee, X.-Y. Gao, X.-D. An, C.-H. Chan, C.-T. Yip, H.-Y. Deng, and C.-H. Lam, *Physical Review Letters* **129**, 168002 (2022).
- [48] C. Cammarota and G. Biroli, *Proceedings of the National Academy of Sciences* **109**, 8850 (2012).
- [49] L. Berthier, D. Coslovich, A. Ninarello, and M. Ozawa, *Physical review letters* **116**, 238002 (2016).

- [50] G. Biroli and J.-P. Bouchaud, *Comptes Rendus. Physique* **24**, 1 (2023).
- [51] D. Chandler and J. P. Garrahan, *Annual review of physical chemistry* **61**, 191 (2010).
- [52] C. Scalliet, B. Guiselin, and L. Berthier, *Physical Review X* **12**, 041028 (2022).
- [53] T. W. de Geus, A. Rosso, and M. Wyart, arXiv preprint arXiv:2401.09830 (2024).
- [54] L. Berthier, G. Biroli, J.-P. Bouchaud, and G. Tarjus, *J. Chem. Phys.* **150**, 094501 (2019).
- [55] P. Charbonneau, J. Kurchan, G. Parisi, P. Urbani, and F. Zamponi, *J. Stat. Mech.* **2014**, 10009 (2014).
- [56] T. Maimbourg, J. Kurchan, and F. Zamponi, *Phys. Rev. Lett.* **116**, 015902 (2016).
- [57] G. Biroli, J.-P. Bouchaud, A. Cavagna, T. Grigera, and P. Verrocchio, *Nat. Phys.* **4**, 771 (2008).
- [58] J. Kurchan and L. Laloux, *J. Phys. A* **29**, 1929 (1996).
- [59] G. Biroli, J.-P. Bouchaud, K. Miyazaki, and D. Reichman, *Phys. Rev. Lett.* **97**, 195701 (2006).
- [60] W. Götze, *Complex dynamics of glass-forming liquids: A mode-coupling theory*, Vol. 143 (OUP Oxford, 2008).
- [61] A. Widmer-Cooper, P. Harrowell, and H. Fynewever, *Physical review letters* **93**, 135701 (2004).
- [62] R. M. Alkemade, E. Boattini, L. Filion, and F. Smalenburg, *The Journal of Chemical Physics* **156**, 204503 (2022).
- [63] S. S. Schoenholz, E. D. Cubuk, E. Kaxiras, and A. J. Liu, *Proceedings of the National Academy of Sciences* **114**, 263 (2017).
- [64] C. Toninelli, G. Biroli, and D. S. Fisher, *Physical review letters* **96**, 035702 (2006).
- [65] A. S. Keys, L. O. Hedges, J. P. Garrahan, S. C. Glotzer, and D. Chandler, *Physical Review X* **1**, 021013 (2011).
- [66] F. Puosi and D. Leporini, *The Journal of chemical physics* **136**, 041104 (2012).
- [67] L. Berthier, G. Biroli, D. Coslovich, W. Kob, and C. Toninelli, *Physical Review E* **86**, 031502 (2012).

Appendix A: Numerical Details

We use for system sizes $N_{d=2} = 484$ and $N_{d=3} = 512$, which allow to perform extensive simulations as ϕ , f_P and f_R are varied, while having small finite-size effects for the dynamical range considered [67]. Our Monte Carlo algorithm follows previous choices [41]: it involves displacements and swap moves, where the latter are attempted with a probability of 20%. The magnitude δl of translation moves is chosen such that the acceptance ratio is 75%.

To achieve rapidly equilibration for any choice of (ϕ, f_R, f_P) , we first use our fastest Monte Carlo, corresponding to $(\phi, f_R = 0, f_P = 0)$. Then our algorithm is run with the desired values of (f_R, f_P) for 10^9 Monte Carlo steps. To check that equilibration was reached, we compare relevant observables (such as correlation functions) in the first and second half of the run, and test for consistency.

The magnitude of the effect of the SWAP in speeding up the dynamics is affected by the width of the particle radii distribution. The degree of polydispersity is quan-

tified as in [41] by some quantity $\delta = \sqrt{\langle \sigma^2 \rangle - \langle \sigma \rangle^2} / \langle \sigma \rangle$, where $\langle \sigma \rangle$ is the average diameter of the packing which our unit length. In this work we use packings with sizes distribution shown in Fig. 4, which have polydispersity 19% and 23% for $d = 2$ and $d = 3$ respectively.

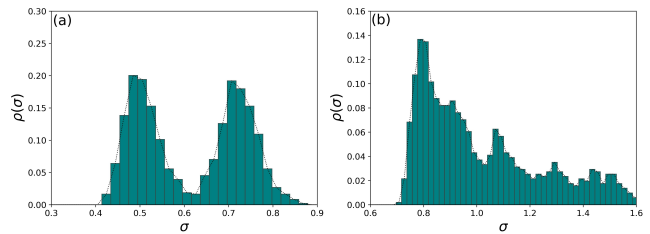


FIG. 4: Initial radius distribution for the (a) 2D system and (b) 3D system.

Appendix B: The effect of the continuous swap

In order to characterize the dynamics of the system for $d = 3$ we consider the usual self-scattering correlation function $F_s(k, t) = \langle \frac{1}{N} \sum_i e^{i\mathbf{k} \cdot [\mathbf{r}_j(t) - \mathbf{r}_j(0)]} \rangle$, where $\mathbf{r}_j(t)$ is the position of the particle j at time t and the wave vector \mathbf{k} satisfies $|\mathbf{k}| = 2\pi/(\sigma)$. For $d = 2$, this definition is not well-suited (long-wavelength vibrational modes bring $F_s(k, t)$ to zero for large t and N , even in a crystal). This problem is fixed as is usually done by considering the relative motion of particle with respect to their neighbors. It can be achieved by introducing the correlation $C(t) = \frac{1}{N} \sum_i C^i(t)$, with $C^i(t) = \frac{1}{n_i(t)} \sum_{\langle ij \rangle} W(1 - \frac{|\mathbf{r}_j(t) - \mathbf{r}_j(t_0) - (\mathbf{r}_i(t) - \mathbf{r}_i(t_0))|}{\langle R \rangle})$ where $\langle R \rangle$ is the average radius of the particles, $n_i(t)$ is the number of neighbors of the particle i at time t defined as all particles j for which $|\mathbf{r}_j(t) - \mathbf{r}_i(t)| < 2.4\langle R \rangle$, an estimate of the first shell of neighbors, and $W(x)$ is the Heaviside function. To extract a relaxation time τ_α , $F_s(k, t)$ and $C(t)$ are fitted with an stretched exponential function $f(t) = \exp(-(t/\tau_\alpha)^\beta)$, where τ_α is the relaxation time. The glass packing fraction $\phi_G(f_R, f_P)$ is then defined such that $\tau_\alpha = \tau_\alpha^* \equiv 10^7$ Monte Carlo steps per particle. The associated stretch exponents β_G are reported in the Appendix as a function of (f_R, f_P) .

Speed up: For $d = 3$, our choice of polydispersity and Monte-Carlo algorithm follows closely previous works [41, 49], where it was shown that swap can speed up the dynamics by 15 decades or more. Here we observe a giant speed up in our $d = 2$ system as well, that continuously builds up as f_R decreases toward the swap case $f_R = 0$ starting from the normal dynamics $f_R = 1$. Fig.5, in Appendix B, shows the relaxation times τ_α - extracted from correlation functions as recalled in Appendix C - as a function of the packing fraction ϕ for different values of f_R . It is notable that τ_α depends very significantly on f_R , but that this dependence is continuous. Finally, the speed-up of swap can be approx-

imately extrapolated to the case where the normal dynamics would reach experimental time scales (i.e. would increase by 15 decades). The range of the corresponding ϕ_G^{exp} can be estimated by fitting the curve $\tau_\alpha(\phi)$ of the normal dynamics $f_R = 1, f_P = 0$ with plausible functional forms for $\tau_\alpha(\phi)$. The functional forms used to fit $\tau_\alpha(\phi)$ and estimate ϕ_G^{exp} are the Vogel-Fulcher-Tamman $\tau_\alpha \sim \exp\left(\frac{A}{\phi_{VFT} - \phi}\right)$ or a form with non-singular activation energy $\tau_\alpha = \tau'_\infty \exp(A'(\phi_c - \phi)^2)$. In agreement with previous such inferences [41, 49], we obtain that the swap dynamics $f_R = 1$ has only slowed-down by 3 to 6 decades at ϕ_G^{exp} : the speed up conferred by swap is very high.

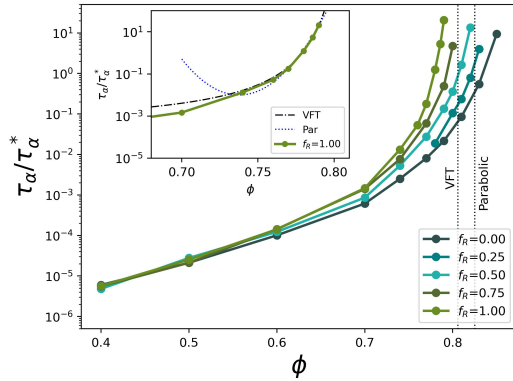


FIG. 5: $\tau_\alpha / \tau_\alpha^*$ as a function of ϕ for a two-dimensional system for different values of f_R . The dotted lines shows the values of ϕ_{VFT} and ϕ_P obtained by fitting the normal dynamics simulation ($f_R = 1$). These fits are shown the insert panel.

Appendix C: Stretched exponents

Figures 6-(a,b) show β_G in color as a function of f_R and f_P for 2D and 3D system respectively where β_G is the value of β obtained at ϕ_G . These values were obtained

through the fitting of function $F_s(k, t)$ and $C(t)$ with an stretched exponential function $f(t) = \exp(-(t/\tau_\alpha)^\beta)$, where τ_α is the relaxation time. In both cases β_G decreases as the system becomes more restricted.

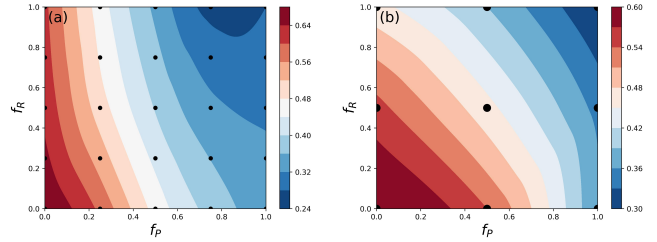


FIG. 6: β_G as a function of f_R and f_P for $d = 2$ (a) and $d = 3$ (b). The color-code represents the value of β_G .

Appendix D: Measure of $l_c(t)$

To define a coarsening length $l_c(t)$, we first define relaxed particles. Particle i is a relaxed particle if $C^i(t) \leq 0.5$. Recall that $C^i(t)$ represents the proportion of particles j that remain neighbors of particle i after a time t . Then we consider that two relaxed particles i and j belong to the same cluster if $|\mathbf{r}_j(t) - \mathbf{r}_i(t)| < 2.4(R)$. An example of a growing length scale is presented in Fig.(7) where relaxed particles are shown in red.

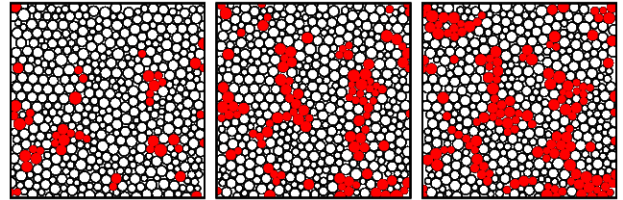


FIG. 7: Spatio-temporal evolution of the structural relaxation in a 2d, $f_R = 0, f_P = 0$ and $\phi = 0.79$, for which $\tau_\alpha = 2.6 \times 10^5$. Red color indicates relaxed particles. From left to right, the snapshots are taken at times $\tau_\alpha/10$ ($l_c \approx 2.7$), $\tau_\alpha/5$ ($l_c \approx 4.5$) and $\tau_\alpha/4$ ($l_c \approx 5.7$).